Ferrimagnetic Behavior of *meso*-Tetrakis(2,3,5,6-tetrafluoro-4-methoxyphenyl)porphyrinatomanganese(III) tetracyanoethenide, $[MnTF_4OMePP][tcne]\cdot 2PhMe$: Structural Evidence for a Second-Order Crystallographic Phase Transition

Durrell K. Rittenberg,[a] Ken-ichi Sugiura,[b] Yoshiteru Sakata,[b] Ilia A. Guzei,[c] Arnold L. Rheingold,[c] and Joel S. Miller*[a]

Abstract: The reduction of *meso*-tetrakis(pentafluorophenyl)porphyrinatomanganese(III) chloride, $Mn^{III}TF_5PPCl$, with methanolic sodium borohydride and subsequent reaction with tetracyanoethylene, TCNE, leads to formation of the magnet *meso*-tetrakis[2,3,5,6-tetrafluoro-4-methoxyphenyl]porphyrinatomanganese(III) tetracycanoethanide, $[Mn^{III}TF_4OMePP]^+[tcne]^{\bullet -}\cdot 2PhMe$, which has been characterized by single-crystal X-ray diffraction, magnetic, and thermal measurements. The structure undergoes a reversible phase transition below $-100\,^\circ C$ (173 K) and the structure was solved and refined in a monoclinic unit cell both at $-45\,^\circ C$ (228 K) [$P2_1/n$, $a = 9.3926(2)$, $b = 25.3254(4)$, $c = 13.2053(2)$ Å, $\beta = 97.203(2)^\circ$, $V = 3116.37(10)$ Å^3, $\rho_{calcd} = 1.478\ g\,cm^{-3}$, $Z = 2$, 4019 reflections, $R1(F_o) = 0.0743$ for the data with $F > 2\sigma(F)$ and 0.0871 for all data], and $-179\,^\circ C$ (94 K) [$P2_1/a$, $a = 14.8410(5)$, $b = 25.366(1)$, $c = 16.7333(5)$ Å, $\beta = 108.091(2)^\circ$, $V = 5987.91$ Å^3, $\rho_{calcd} = 1.540\ g\,cm^{-3}$, $Z = 4$, 11792 reflections, $R(F_o) = 0.069$ for the data with $F > 3\sigma(F)$]. $[Mn^{III}TF_4OMePP][tcne]\cdot 2PhMe$ has a linear chain (1D) coordination polymer motif composed of alternating $[Mn^{III}TF_4OMePP]^+$ cations and bridging $[tcne]^{\bullet -}$. At $-45\,^\circ C$ the one-dimensional (1D) chain is uniform with an $Mn{-}N_{TCNE}$ distance of 2.320(4) Å, whereas at $-179\,^\circ C$ the 1D chain is nonuniform with $Mn{-}N_{TCNE}$ distances of 2.291(2) and 2.283(2) Å and the $[tcne]^{\bullet -}$ ion is disordered over two orientations in a 79:21 ratio. This is the first time that this slight chain nonuniformity has been observed for a magnetically ordered system. The crystallographic phase change that occurs between -100 and $-162\,^\circ C$ was not observed in the magnetic or thermal studies. Hence, structures should be determined at the lowest possible temperature, to enhance confidence that a reliable structure–property relationship can be obtained. The temperature dependence of the magnetic susceptibility above 200 K could be fitted to a Curie–Weiss expression with an effective θ (θ') of 93 K. Intrachain coupling was modeled to a Seiden expression ($H = -2\boldsymbol{S}_a\cdot\boldsymbol{S}_b$) with a J_{intra} of -235 K ($-163\ cm^{-1}$; $326\ cal\,mol^{-1}$; 29 meV) and 10 Hz ac magnetic susceptibility, indicating an ordering temperature, T_c, of 10.3 K. The frequency dependence of the ac susceptibility indicates spin glass behavior.

Keywords: chain structures · magnetic properties · metalloporphryins · phase transitions · structure elucidation

Introduction

The preparation of molecule-based magnetic materials is a growing area of contemporary interdisciplinary research.[1, 2] Variations in the first organic-containing molecule-based magnet to be characterized, the electron-transfer salt $[FeCp^*]^+[tcne]^{\bullet -}$ ($Cp^* =$ pentamethylcyclopentadienide; tcne = tetracyanoethylene), with an ordering temperature (T_c) of 4.8 K,[3] led to the discovery of the first room-temperature molecule-based magnet, the disordered $V[tcne]_x\cdot y$(solvent) with a T_c of approximately 400 K.[4] More recently, studies have focused on a class of metallomacrocycles and $[tcne]^{\bullet -}$-based magnets exemplified by $[MnTPP][tcne]\cdot 2PhMe$ (TPP = *meso*-tetraphenylporphyrinato) with a T_c of 14 K.[5] Since then additional porphryin-

[a] Prof. J. S. Miller, D. K. Rittenberg
Department of Chemistry, 315 S. 1400 E. RM Dock, University of Utah
Salt Lake City, UT 84112–0850 (USA)
Fax: (+1) 801-581-8433
E-mail: jsmiller@chemistry.utah.edu

[b] Prof. Y. Sakata, Dr. K. Sugiura
Institute of Scientific and Industrial Research, Osaka University
Yamadakami, Suita, Osaka 565 (Japan)
Fax: (+81) 6-87-8479
E-mail: sakata@sanken.osaka-u.ac.jp;
sugiura@sanken.osaka-u.ac.jp

[c] Prof. A. L. Rheingold, I. A. Guzei
Department of Chemistry, University of Delaware
Newark, DE 19716 (USA)
Fax: (+1) 302-831-6335
E-mail: arnrhein@udel.edu

0947-6539/99/0506-1874 $ 17.50+.50/0 *Chem. Eur. J.* **1999**, *5*, No. 6

based magnets have been prepared and characterized, although the origin of the magnetic behavior of this class of materials is still under investigation.[6] With the hope of establishing a structure–function relationship, our group and others have prepared a series of substituted tetraphenylporphryin–TCNE complexes.[6–10]

As it is relatively easy to modify the porphryin structure, we sought to prepare highly electron-deficient porphyrins[7] by introducing halogen atoms on the phenyl groups appended to the porphyrin. The effect of the electronic properties of the porphyrin on the intrachain coupling is not fully understood, but it has been suggested that the degree of electron transfer controls the intrachain coupling and consequently the magnitude of T_c.[10a] However, this control unlikely to predominate in the solid state as the phenyl substituents, which control the redox properties, are perpendicular to the porphyrin ring, thus effectively minimizing their electronic contribution. Furthermore, different solvates have different magnetic behavior which cannot be ascribed to differing degrees of electron transfer.[7e]

In contrast, we have shown that the strength of intrachain coupling correlates inversely with the dihedral angle between the $[tcne]^{\bullet-}$ and the porphyrin mean planes, and with the Mn-N-C angle, due to the strength of the $\sigma-p_z/d_{z^2}$ overlap.[11] Efforts to control the crystal packing to induce more strongly magnetically coupled systems with reduced angles in this class of materials prompted us to prepare highly substituted, [manganese(III)porphyrin][tcne] salts. We report the structure and magnetic properties of *meso*-tetrakis(2,3,5,6-tetrafluoro-4-methoxyphenyl)porphyrinatomanganese(III) tetracyanoethenide ([$MnTF_4OMePP$][tcne], **1**[tcne]). We also give the first description for this class of materials of a thermally induced second-order crystallographic phase transition.

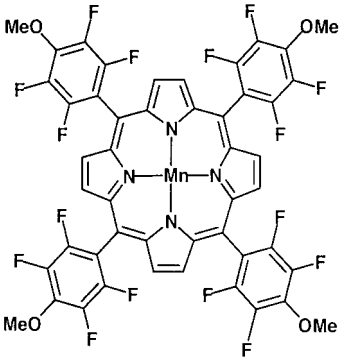

$MnTF_4OMePP$, **1**

Results and Discussion

$Mn^{III}TF_5PPCl$ was prepared from the corresponding free base[12] by a previously reported method.[13] The reduction of $Mn^{III}TF_5PPCl$ with $NaBH_4$ in a MeOH/pyridine mixed-solvent system led to a purple metalloporphyrin, which was subsequently determined by a single-crystal X-ray diffraction study to contain **1**. Facile nucleophilic substitution of the *p*-fluorine with methoxide from the slow reaction of $NaBH_4$ in MeOH occurs unexpectedly in this system, although it has also been reported for alkylamines and alkoxides.[14] This suggests that long-chain alcohols might be used to form liquid-crystalline, 2,3,5,6-tetrafluorophenyl-substituted porphyrins.

The resulting $Mn^{II}TF_4OMePPpy$ reacts with TCNE in toluene to form [$MnTF_4OMePP$][tcne]·2PhMe. Attempts to prepare [$MnTF_5PP$][tcne] by the reaction of H_2TCNE/TCNE (1:1) and $Mn^{III}TF_5PPOAc$, analogously to the method used to prepare [MnTP′P][tcne],[7a] [H_2TP′P = tetrakis(3,5-di-*tert*-butyl-4-hydroxyphenyl)porphyrin], and the reduction with a stoichiometric amount of lithium triethylborohydride (superhydride) led to impure products.

The IR absorption maxima at $\tilde{\nu}(CN) = 2126$ (s) and 2194 (m) cm^{-1} confirm the presence of coordinated $[tcne]^{\bullet-}$ and do not indicate $[tcne]^{n-}$ ($n = 0, 2$).[15] The high-energy absorption at 2126 (s) cm^{-1} is at considerably lower frequency than that reported for [MnTPP][tcne], 2147 (s) cm^{-1}.[5] Variable-temperature IR spectroscopy over the range 17–373 K showed no evidence for a phase transition, indicating that the transition is not observable by IR spectroscopy. However, a decrease in intensity of the peak at 2126 cm^{-1} which began above 373 K was accompanied by the appearance of a new peak at 2135 cm^{-1}, associated with formation of a desolvated phase, which persisted upon cooling. Further differential scanning calorimetry (DSC) measurements over the range −170 to 50 °C showed no evidence of a thermal event. Thermogravimetric analysis coupled with mass spectrometry (TGA/MS) of **1**[tcne]·2PhMe showed a single weight loss of 12.81% corresponding to a loss of 1.67 PhMe (m/z 91) between 116 and 123 °C. Deviations from the predicted values of 2 PhMe units per formula unit observed in the crystal structure and 1.75 PhMe predicted by elemental analysis are probably due to solvent losses during sample handling and are typical for this class of materials.[7]

Structure: The single-crystal X-ray structure of **1**[tcne] was determined at −45 (α-phase) and −179 °C (β-phase) (Table 1, Figure 1). Unexpectedly, the structures were not isomorphous at these temperatures. Since these structures were determined independently on different crystals, the possibility became evident that two polymorphs of the same material existed and that the physical properties of each phase should be studied independently.[16] The unit cell of another crystal, determined

Table 1. Crystallographic data for α- and β-[$MnTF_4OMePP$][tcne]·2PhMe.

	α-phase	β-phase
formula	$C_{68}H_{36}N_8MnF_{16}O_4$	$C_{68}H_{36}N_8MnF_{16}O_4$
formula weight	1388.00	1388.00
space group	$P2_1/n$ (no. 14 b2)	$P2_1/a$ (no. 14 b3)
a [Å]	9.3926(2)	14.8410(5)
b [Å]	25.3254(4)	25.366(1)
c [Å]	13.2053(2)	16.7333(5)
β [°]	97.203(2)	108.091(2)
Z	2	4
V [Å^3]	3166.37(10)	5987.91(2)
ρ_{calcd} [g cm^{-1}]	1.487	1.540
$R(F_o)$	0.073 (7.3%)	0.069 (6.9%)
$R_w(F_o)$	0.2076	0.073
Temperature [°C]	−45	−179
λ [Å]	0.710730	0.710730

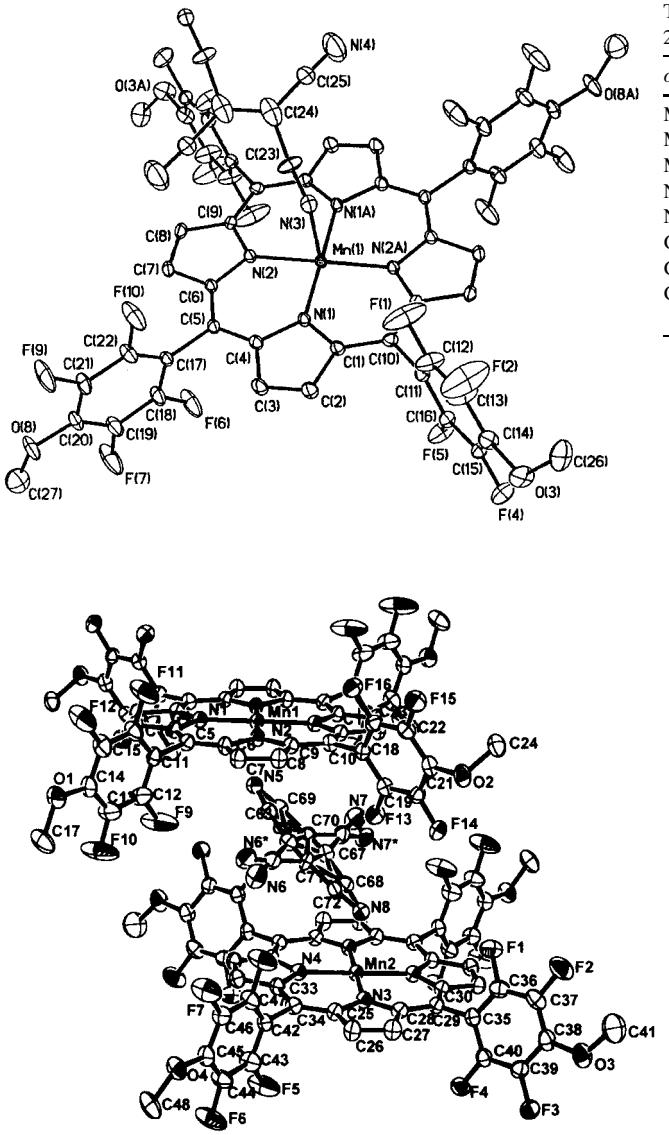

Figure 1. ORTEP (30%) atom labeling diagrams for α-[$MnTF_4$OMePP][tcne]·2PhMe (top) and β-[$MnTF_4$OMePP][tcne]·2PhMe (bottom). Note the disordered $[tcne]^{\bullet-}$ in the β-phase.

Table 2. Selected interatomic distances [Å], for α- and β-[$MnTF_4$OMePP][tcne]·2PhMe.

α-Phase		β-Phase (major, minor)	Major form	Minor form
Mn(1)–N(3)	2.320(4)	Mn(1)–N(5), Mn(2)–N(8)	2.283(2)	2.291(2)
Mn(1)–N(1)	2.019(3)	Mn(1)–N(1)	2.016(3)	
Mn(1)–N(2)	2.015(4)	Mn(1)–N(2)	2.018(3)	
N(3)–C(23)	1.146(7)	N(5)–C(63), N(5)–C(69)	1.177(7)	1.18(2)
N(4)–C(25)	1.133(9)	N(7)–C(66), N(7*)–C(66)	1.153(7)	1.18(2)
C(23)–C(24)	1.514(11)	C(63)–C(64), C(69)–C(70)	1.395(8)	1.39(5)
C(24)–C(24′)	1.30(2)	C(64)–C(67), C(70)–C(71)	1.425(8)	1.44(2)
C(24)–C(25)	1.394(9)	C(64)–C(65), C(71)–C(65)	1.425(6)	1.42(1)
		C(66)–C(67), C(66)–C(70)	1.416(6)	1.44(1)

Table 3. Selected intramolecular angles [°] for α- and β-[$MnTF_4$OMePP][tcne]·2PhMe.

	α-Phase		β-phase
N(3)-C(23)-C(24)	173.4(7)	N(5)-C(63)-C(64), major	177.0(6)
		N(5)-C(69)-C(70), minor	174(1)
Mn(1)-N(3)-C(23)	124.9(4)	Mn(1)-N(5)-C(63), major	123.0(1)
		Mn(2)-N(8)-C(68), major	120.0(1)
		Mn(1)-N(5)-C(69), minor	125.3(1)
		Mn(2)-N(8)-C(72), major	123.0(1)
C(23)-C(24)-C(25)	118.8(7)	C(63)-C(64)-C(65)	119.2(5)
		C(69)-C(70)-C(66)	117(1)

at −100 °C, was found to be the same as that determined at −45 °C [$a = 9.301(17)$, $b = 25.24(4)$, $c = 12.94(2)$ Å, $\beta = 96.99(16)°$, $V = 3022(16)$ Å^3], while at −162 °C the unit cell parameters [$a = 14.883(5)$, $b = 25.318(10)$, $c = 16.766(5)$ Å, $\beta = 108.39(2)°$, $V = 5995(5)$ Å^3] were the same as those determined at −179 °C. When this material was warmed, its unit cell parameters were comparable with those recorded at −45 °C. Hence, a reversible crystallographic phase transition occurs between −100 and −162 °C. Attempts to identify this phase transition by DSC (above −170 °C) and variable-temperature IR studies (above −140 °C) were unsuccessful (vide supra).

Both phases have Mn located at inversion centers; for the α-phase the $[tcne]^{\bullet-}$ is also at an inversion center, but for the β-phase the $[tcne]^{\bullet-}$ centroids are not in a special position. Furthermore, there are two crystallographically distinct Mn centers for the β-phase. The planar cation is comparable with other [Mn^{III}(porphyrin)] complexes reported in the literature,[5–7, 17] with average Mn–N distances of 2.017 Å for both phases (Tables 2 and 3).

The $[tcne]^{\bullet-}$ ion is ordered for the α-phase; the central C–C bond length is 1.30(2) Å. This is shorter than the 1.344(4) Å reported for TCNE,[15a] whereas 1.39 Å is expected for $[tcne]^{\bullet-}$ ion.[15b] Since $[tcne]^{\bullet-}$ lies at an inversion center, this distance is symmetry-generated and, if the crystallographic symmetry is higher than the molecular symmetry, unresolved disorder in the $[tcne]^{\bullet-}$ may lead to the unpredicted short bond length. The ν(CN) absorption is characteristic of $[tcne]^{\bullet-}$, but not TCNE. In contrast, disordered $[tcne]^{\bullet-}$ is resolved in the β-phase; it has two orientations, in a 71:29 ratio, in the same plane with the minor orientation rotated by 90° relative to the major orientation. This type of disorder has been observed for [MnTPP][tcne]·2PhMe[18] and its *o*-fluoro-substituted analogue.[7f] The average central C–C bond length for the two orientations is 1.43 Å, as expected for its bond order of 1.5.[15]

As has been observed for several related materials, both phases are composed of parallel 1-D $\cdots D^+A^{\bullet-}D^+A^{\bullet-}\cdots$ polymer chains {D = [$MnTF_4$OMePP]$^+$; A = $[tcne]^{\bullet-}$}, where the $[tcne]^{\bullet-}$ is *trans*-μ-*N*-σ-bonded to two Mn^{III} atoms, each at an inversion center (Figures 2 and 3). In contrast to the α-phase, the β-phase has two crystallographically independent porphyrin macrocycles, each essentially identical, yielding a pseudo-uniform chain structure. The $MnTF_4$OMePP units are parallel to each other for the α-phase, but have a dihedral angle of 4.16° for the β-phase. The details of the interchain structure differ from those reported earlier[7, 8] with the exception of [MnPc][tcne][19a] (H_2Pc = phthalocyanine) and [MnOEP][tcne][19b] (H_2OEPc = octaethylporphyrin), which exhibit stronger intrachain dimerization and lack magnetic ordering. This is the first time that a slight deviation from a

0947-6539/99/0506-1876 $ 17.50+.50/0 *Chem. Eur. J.* **1999**, *5*, No. 6

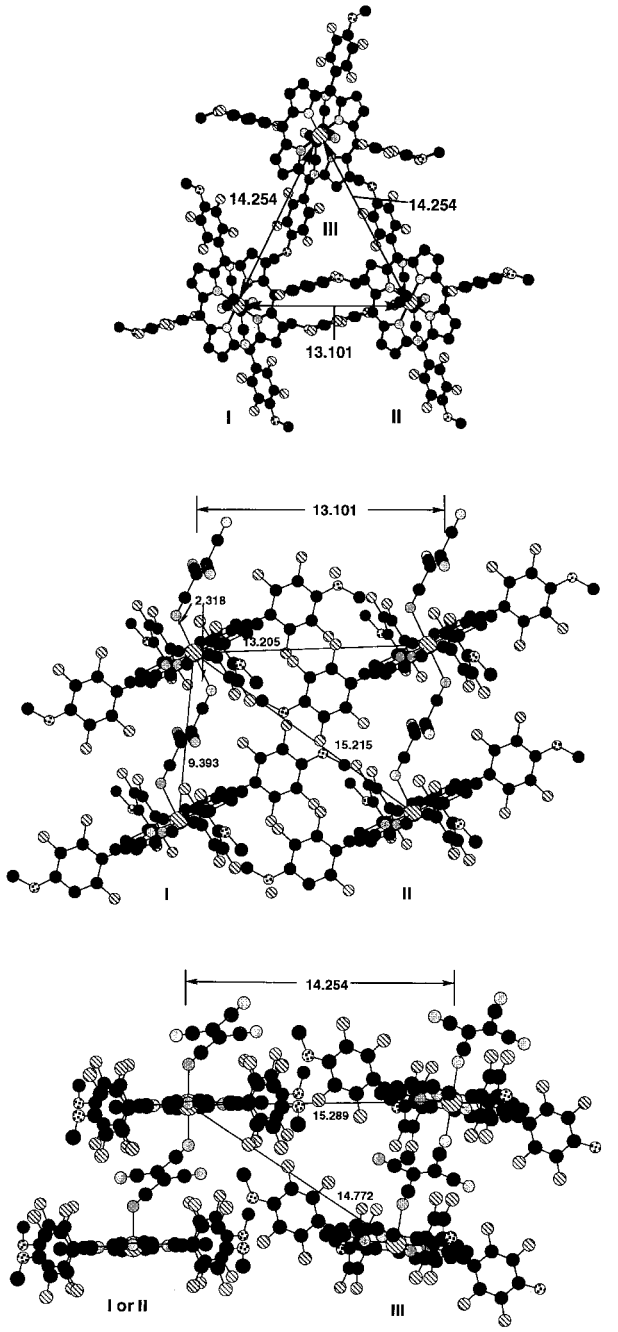

Figure 2. Views of interchain interaction among the unique chains **I**, **II**, and **III** for α-[$MnTF_4OMePP$][tcne]·2PhMe (the solvent is omitted for clarity).

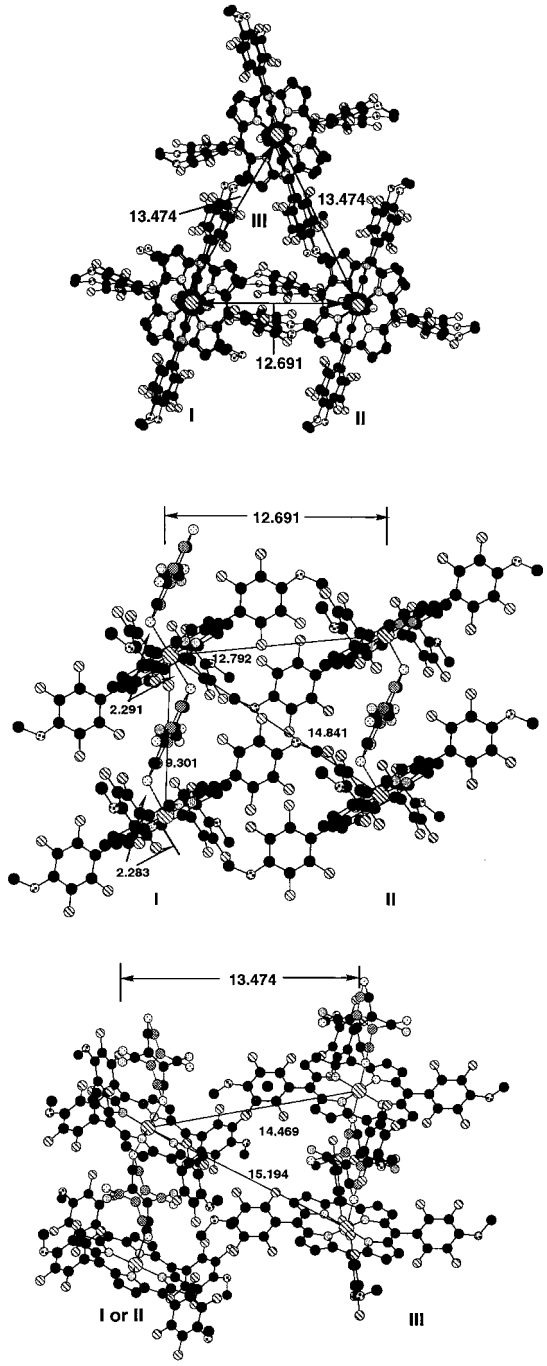

Figure 3. Views of interchain interaction among the unique chains **I**, **II**, and **III** for β-[$MnTF_4OMePP$][tcne]·2PhMe (the solvent is omitted for clarity).

nonuniform chain motif has been observed for a magnetically ordered system.

The Mn–N_{TCNE} bond lengths were found to be 2.320(4) Å for the α-phase and 2.283(2) Å and 2.291(2) Å (av 2.287 Å) for the β-phase. The shorter Mn–N distance at $-179\,^{\circ}C$ is expected because of the contraction of the unit cell at lower temperatures. The Mn–N bond length at $-45\,^{\circ}C$ is slightly longer than that in [MnTPP][tcne] at 173 K (2.306 Å)[5a] and [MnTP*P][tcne] at 208 K (2.299 Å).[7a] The intrachain Mn···Mn separations are 9.393 Å (α-phase) and 9.301 Å (β-phase) and fall within the range of known [Mn(porphyrin)][tcne] structures.[6, 7] The Mn-N-C_{TCNE} angle and the dihedral angles between the MnN_4 and $(NC)_2C$ mean planes are 124.9° and 33.4° for the α-phase and 124.1° (121.5°), and 31.2° (34.7°) for the major (and minor) forms of the β-phase. These values are comparable with those for [MnTP*P][tcne]·2PhMe (129.0 and 33.60),[5, 18] but significantly lower than those for [MnTPP][tcne]·2PhMe (146.8° and 55.4°).[5, 7a] The low values of the dihedral and Mn-N-C angles suggest strong intrachain coupling and large values of θ' due to enhanced overlap of the π^* orbital on nitrogen with the spin coupling d_{z^2} orbital of Mn;[11] thus the predicted θ' of approximately 90 K

is in good agreement with the observed value of 93 K (vide infra). The nearest neighbor interchain interactions for the α- and β-phases of [MnTPP][tcne]·2PhMe are depicted in Figures 2 and 3. Each member of the [Mn(porphyrin)][tcne] family[6, 7] is composed of parallel 1-D $\cdots D^{+}A^{\bullet -}D^{+}A^{\bullet -}\cdots$ chains, but the intrachain interactions in [MnTPP][tcne]·2PhMe are unusual in comparison with the other family members. For both the α- and the β-phases a herringbone arrangement exists between adjacent chains. Similar packing was observed in [MnTClPP][tcne]·$2CH_2Cl_2$;[7e] however, [MnTPP][tcne]·2PhMe is the first toluene solvate found to crystallize with this motif.

The key interchain Mn···Mn distances in the α- and β-phases (Figures 2 and 3) range from 13.205 to 20.635 Å and 12.792 to 20.465 Å, respectively. Thermal contractions between phases range from 0.53 to 3.13% (interchain) and 0.82 to 4.9% (intrachain) (Table 4). The most dramatic differences were found for the $F\cdots N_{TCNE}$ interactions, which changed by 4.9 and 17.9% for the major and minor orientations, respectively.

Table 4. Selected interchain and close contact distances [Å] for α- and β-[$MnTF_4OMePP$][tcne]·2PhMe

Mn–Mn	α-Phase	β-Phase	Δ Distance [%]
A (chain Ib – Ia)	13.206	12.792	3.13
B (chain Ib – IIa)	14.773	14.694	0.53
C (chain Ib – IIa)	15.290	15.194	0.62
D (chain IIb – Ia)	19.471	19.339	0.67
E (chian IIb – Ib)	20.635	20.465	0.82
C≡N···F	3.721, 3.703	3.535, 3.524 (major)	4.9, 4.8 (major)
		3.138, 3.038 (minor)	14.5, 17.9 (minor)

The origin of the $[tcne]^{\bullet -}$ rotational disorder, which is present only in the β-phase, may be a favorable N6 – F19 interaction; the 17.9% decrease in the N6 – F19 distance from 3.721 to 3.058 Å which occurs upon cooling is larger than expected for thermal contraction of the lattice. This interaction was also observed in [MnTFPP][tcne][7f], which exhibits close $F\cdots N_{TCNE}$ contacts of 3.318 Å at −45 °C. To the best of our knowledge this interaction is unprecedented.

Magnetic behavior: The temperature dependence from 2 to 300 K of the reciprocal magnetic susceptibility, χ, and effective magnetic dipole moment, μ_{eff}, can be fitted above 200 K to a Curie – Weiss expression, $\chi = 1/(T-\theta')$, with an effective θ, θ',[7e,f] of 93 K (Figure 4). This value is significantly higher than that of [MnTPP][tcne] (61 K) and close to that of [MnTP*P][tcne] (90 K); it is the highest θ' value reported to date for this class of materials, indicating very strong intrachain coupling. The room-temperature effective moment, μ_{eff} $\{\equiv[8\chi T]^{1/2}\}$, is 5.61 μ_B, significantly higher than the expected 5.20 μ_B for an anisotropic independent system with $g=2$, $S=2$, and $S=½$,and arises from strong effective ferromagnetic coupling.

The χT(T) data can be fitted to the Seiden expression for noninteracting chains composed of alternating quantum ($S=½$) and classical ($S>½$) spins[20] using the Hamiltonian $\mathscr{H} = -2J\boldsymbol{S}_i\cdot\boldsymbol{S}_j$ with $J/k_B = -235$ K (-163 cm^{-1}; 326 cal mol^{-1}; 29 meV) (k_B = Boltzmann's constant) consistent with ferri-

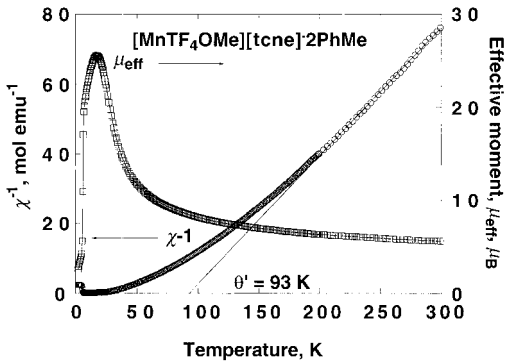

Figure 4. Reciprocal molar magnetic susceptibility, χ^{-1}, and effective dipole moment, μ_{eff}, as a function of temperature for polycrystalline [$MnTF_4OMePP$][tcne]·2PhMe.

magnetic behavior assuming $g_{Mn^{III}} = g_{[tcne]^{\bullet -}} = 2.002$ (Figure 5). This J value reflects the strong intrachain antiferromagnetic coupling. A fit to the Seiden function predicts a broad minimum at 975 K, which cannot be verified. The data below 70 K exceed the predicted value for a purely 1D system,

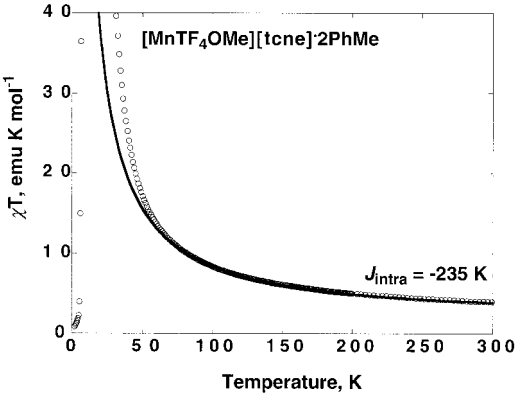

Figure 5. $\chi T(T)$ for [$MnTF_4OMePP$][tcne]. Data were collected in a 1000 Oe field. The solid line represents a fit to the predictions for alternating quantum/classical spin ferrimagnetic chains (see text).

indicating that ferromagnetic coupling between chains begins to dominate, as observed for other [manganoporphryin][tcne] magnets.[21] Previously, inverse correlations of the dihedral angle between the MnN_4 and the $(NC)_2C$ mean planes, and of the Mn-N-C angle, with the magnitude of the intrachain coupling, θ', were established, with lower values of these angles correlating with larger values of θ',[11] and stronger intrachain coupling was observed. A θ' value of approximately 90 K is predicted from the data, in good agreement with the observed value of 93 K (vide supra).

Antiferromagnetic behavior is also evident from the magnetization data. The 2 K isothermal magnetization increases gradually with increasing applied field below 27 kOe, after which it rises rapidly to near-saturation, M_s (Figure 6). At 5 T and 2 K the magnetization is 16560 emu Oe mol^{-1}, in good agreement with the 16755 emu Oe mol^{-1} expected for an antiferromagnetically coupled $S_{Tot} = 2 - ½ = 3/2$ system. This is substantially lower than the value expected from ferromagnetic coupling, that is, 27925 emu Oe mol^{-} for an

0947-6539/99/0506-1878 $ 17.50+.50/0 Chem. Eur. J. 1999, 5, No. 6

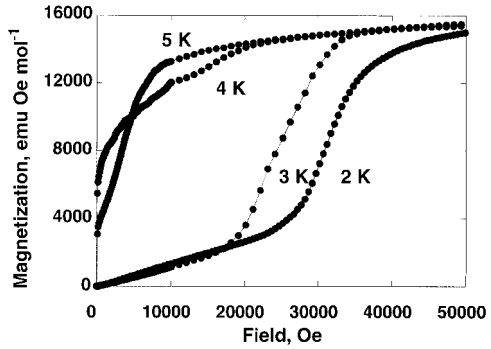

Figure 6. Variable-temperature saturation magnetization for a polycrystalline sample of $[MnTF_4OMePP][tcne]$ at 2, 3, 4, and 5 K.

$S_{Tot} = 2 + ½ = 5/2$ system. This metamagnetic behavior (field-induced changeover from an antiferromagnetic ground state to a ferromagnetic ground state) is observed at 2, 3, and 4 K with critical fields, H_c, of 27, 16, and 0.5 kOe, respectively. Above 5 K **1**[tcne] behaves as a ferromagnet; therefore the critical temperature of the metamagnetic transition is approximately 5 K. Similar field dependence has been observed for $[MnTPP][tcne]\cdot 2PhMe$, which exhibits an H_c of approximately 30 kOe at 2.25 K corresponding to a spin–flop transition.[5b] $[MnTF_4OMePP][tcne]\cdot 2PhMe$ exhibits unusual hysteresis behavior that is the focus of ongoing studies.

In addition to dc measurements, the temperature dependence of the in-phase (χ') and out-of-phase (χ'') ac susceptibility was determined in an applied ac field of 1000 Oe (< 0.05 dc field) at several frequencies; the resulting data are consistent with long-range magnetic order. A peak in $\chi'(T)$ at 10 Hz ac susceptibility is a measure of T_c (Figure 7), which

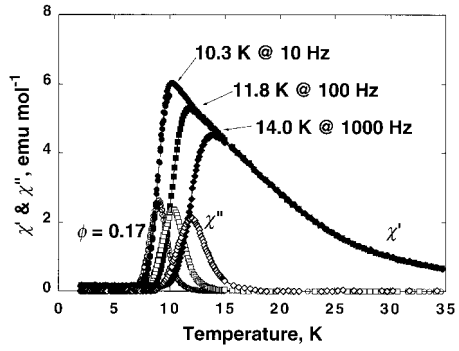

Figure 7. Dispersive, χ', and absorptive, χ'', ac susceptibility as a function of temperature recorded at 10 (●, ○), 100 (▮, □), and 1000 Hz (◆, ◇) for a polycrystalline sample of $[MnTF_4OMePP][tcne]$. Measurements were made in a small applied field of H_{dc}0.1 kOe.

is 10.3 K. This is lower than the values reported for $[MnT'PP][tcne]\cdot 2PhMe$[7a] ($T_c = 15$ K) and $[MnTPP][tcne]\cdot 2PhMe$[5b] ($T_c = 14$ K), but higher than that of $[MnTClPP][tcne]\cdot 2PhMe$ ($T_c = 8.8$ K).[7e] The sample shows significant frequency dependence, indicative of a spin glass state. The disorder parameter, ϕ [$\phi \equiv \Delta T_f/T_f \Delta \log \omega$, where T_f is the freezing temperature, ΔT_f the difference in freezing temperature at the highest and lowest frequencies, and ω the frequency],[22] for $[MnTF_4OMePP]^+[tcne]^{\bullet-}\cdot 2PhMe$ is 0.17; this indicates spin–lattice disorder and suggests that a highly disordered spin glass is formed. It is the highest ϕ value known for the [Mn(porphyrin)][tcne] family of molecule-based magnets[5, 10] and hence $[MnTF_4OMePP]^+[tcne]^{\bullet-}\cdot 2PhMe$ is the most disordered member. Spin glass behavior and disorder in this class of materials are under continuing study.

T_f can also be determined by the divergence of the zero-field cooled magnetization at low field. The positions of the bifurcation points at 0.01, 0.1, and 1 Oe were found to be 7.07, 6.99, and 7.01 K, respectively, which are lower than the 10.3 K observed in the ac experiments.

Conclusion

Substitution of the *p*-fluorine of $Mn^{II}TF_5PP$ by reduction of $Mn^{III}TF_5PPCl$ with $NaBH_4$ in an MeOH/pyridine mixed-solvent system forms $MnTF_4OMePP$ (**1**). This suggests that long-chain alcohols might be used to form liquid-crystalline, 2,3,5,6-tetrafluorophenyl-substituted porphyrins. Reaction of **1** with TCNE forms $[MnTF_4OMePP][tcne]\cdot 2PhMe$, which exhibits strong intrachain coupling as evidenced by θ' (93 K) and J/k_B (-235 K). Surprisingly, the low-temperature β-phase does not consist of a uniform chain; instead, the $Mn1\cdots N_{TCNE}$ and $Mn2\cdots N_{TCNE}$ bond lengths alternate, leading to a short–long–long–short repeat unit at the temperature at which the structure was determined. Other nonuniform chains were observed previously in [MnOEP][tcne][19a] and [MnPc][tcne],[19b] both of which exhibit weak intrachain coupling and not three-dimensional (3D) ordering. Both [MnOEP][tcne] and [MnPc][tcne] have two distinct TCNE units in either ABAB or AABAAB repeat units. β-[MnTF4OMePP][tcne]$\cdot 2PhMe$, however, has only one type of crystallographically equivalent $[tcne]^{\bullet-}$ unit, albeit disordered, in the chain; hence a single J value can describe the system. The structures of [MnOEP][tcne] and [MnPc][tcne] suggest that chain uniformity is needed for magnetic ordering. This is inconsistent with the results reported herein, as the observation of bulk magnetic ordering in $[MnTF_4OMePP][tcne]$ suggests that nonuniform chains can lead to 3D magnetically ordered systems, depending on the nature of the chain nonuniformity. If this observation is true for this class of materials, chains with only one crystallographically unique $[tcne]^{\bullet-}$ unit are necessary for magnetic ordering.

A second possible explanation exists for the 3D ordering: a second crystallographic phase change occurs below 94 K to form a uniform chain again at a lower temperature, and this uniform chain is responsible for the observed order in the sample. A third possibility is that the disordered arrangement observed at 94 K vanishes at low temperature resulting in an ordered structure. Attempts to resolve this issue are in progress.

Regardless of the genesis of the magnetic ordering, this work emphasizes the need to determine the structure at the lowest possible temperature, as the reported structure, even at subambient temperatures, may not represent adequately the structure at the temperature at which interesting physical phenomena occur, and may lead to misleading correlations between the structure and properties. Ideally, structure determinations at liquid-helium temperatures are preferred, but these determinations are not readily obtainable.

Experimental Section

Synthesis: All manipulations were carried out under an atmosphere of nitrogen using standard Schlenk techniques or in a Vacuum Atmospheres DriLab under nitrogen. Solvents used were predried and distilled from appropriate drying agents. H_2TF_5PP was prepared from the condensation of pentafluorobenzaldehyde and pyrrole (Aldrich) by a literature method.[12] TCNE was sublimed before use.

[$MnTF_5PP$]Cl: H_2TF_5PP (513 mg, 0.526 mmol) was added to a suspension of $Mn(OAc)_2 \cdot 4H_2O$ (Sigma) (264.3 mg, 1.02 mmol) in chlorobenzene (50 mL).[13] The mixture was allowed to reflux until thin-layer chromatography (SiO_2) showed no evidence of H_2TF_5PP (> 16 h). The chlorobenzene solution was poured onto a column packed with silica gel, and the product was eluted with chloroform. After the solvent had been removed, the resulting reddish powder was dissolved in a minimum of methanol, aqueous 10% HCl (100 mL) was added, the solution was stirred for 1 h, brine (aq. NaCl) solution (200 mL) was added, and the solid was collected by vacuum filtration. The resulting red-brown material was recrystallized from toluene/hexanes. Yield 485.3 mg (80%), red powder.

$Mn^{II}TF_4OMePPpy$: $NaBH_4$ (650 mg, 17.4 mmol) was added in three portions to a solution of $MnTF_5PPCl$ (350 mg, 0.375 mmol) in pyridine (15 mL) and methanol (20 mL). The solution was heated to reflux for 30 min before being cooled to room temperature. The solvent was removed under reduced pressure to give a crude reddish purple powder that was extracted with toluene. The resulting purple powder was recrystallized from toluene/hexanes. Yield 395 mg (65%), purple crystals.

[$Mn^{III}TF_4OMePP$][tcne]: $MnTF_4OMePPpy$ (135 mg, 0.123 mmol) dissolved in toluene (20 mL) was filtered and added to a solution of toluene (20 mL) and TCNE (17.3 mg, 0.0135 mol). The resulting solution was heated to reflux and immediately cooled to room temperature. After three days large black crystals were observed. The product was isolated by vacuum filtration. Yield 151 mg (85%). IR (Nujol): $\tilde{\nu}(C{\equiv}N) = 2135$ (s), 2193 (m) cm^{-1}. $[MnTF_4OMePP][tcne] \cdot 1.75\,PhMe$ ($MnC_{66.25}H_{34}F_{16}N_8O_4$): calcd.: C 58.30, H 2.51, N 8.21; found: C 58.26, H 2.62, N 8.24. TGA/MS: 12.81% loss of PhMe (m/z: 91), corresponding to 1.92 PhMe per Mn for a different sample.

X-ray structure determination: Crystals suitable for single-crystal X-ray diffraction were obtained by slow diffusion of $MnTF_4OMePPpy$ and TCNE in toluene. The cell constants and orientation matrix for the data collection were obtained by usual methods. A summary of data collection parameters is given in Table 1. Data were collected at $-45\,^{\circ}C$ for the α-phase. Systematic absences in the diffraction data were uniquely consistent with the $P2_1/n$ space group. The structure was solved by direct methods, completed by subsequent difference Fourier synthesis, and refined by full-matrix least-squares procedures. The non-hydrogen atoms were refined with anisotropic displacement coefficients and hydrogen atoms were treated as idealized contributions (Table 1). The Mn atom resides at a crystallographic inversion center, as does the $[tcne]^{\bullet-}$. Data collected at $-179\,^{\circ}C$ for the β-phase gave systematic absences in the diffraction pattern that were uniquely consistent with the $P2_1/a$ space group. They were collected on a Rigaku RAXIS-IV imaging plate area detector system with graphite-monochromated $Mo_{K\alpha}$ radiation (0.71070 Å, 60 kV, 300 mA) to a maximum 2θ of 55.1°. A total of 36 images with oscillation angle 2.50° were collected, each being exposed for 7.0 min. The structure was solved by a direct method. The non-hydrogen atoms were refined anisotropically and the hydrogen isotropically. Unlike the α-phase the $[tcne]^{\bullet-}$ groups do not occupy special positions in the refined structure. Disorder in the orientation and position was observed in the $[tcne]^{\bullet-}$, the details of which are discussed in the text.

Physical methods: The 2–300 K magnetic susceptibility was determined on a Quantum Design MPMS-5XL 5 T SQUID magnetometer (sensitivity = 10^{-8} emu or 10^{-12} emu Oe^{-1} at 1 T) with an ultra-low field (approximately 0.005 Oe) and ac options, using a reciprocating sample measurement system and continuous low-temperature control with enhanced thermometry features. The ac magnetic susceptibility (χ' and χ'') was studied in the range 10–1000 Hz. Samples were loaded in an airtight Delrin holder and packed with oven-dried quartz wool (to prevent movement of the sample in the holder) or in a gelatin capsule. For isofield dc measurements, the samples were zero-field cooled (following oscillation of the dc field), and data were collected upon warming. For dc isothermal and ac measurements, remanent fluxes were minimized by oscillation of the dc field, followed by quenching of the magnet. Remaining fluxes were detected using a flux gate gaussmeter and further minimized by application of an opposing field, to bring the dc field to < 0.5 Oe. The diamagnetic correction of -764×10^{-6} emu mol^{-1} was used for $[MnTF_4OMePP][tcne] \cdot 2\,PhMe$.

The thermal properties were studied on a TA Instruments Model 2050 thermogravimetric analyzer (TGA) equipped with a TA-MS Fison triple filter quadrupole mass spectrometer to identify gaseous products with $m/z < 300$ and located in a Vacuum Atmospheres DriLab under argon to protect air- and moisture-sensitive samples. Samples were placed in an aluminum pan and heated at 20 °C min^{-1} under a continuous 10 mL min^{-1} flow of nitrogen. DSC was performed on a TA Instruments Model 2910 calorimeter equipped with an LNCA liquid-nitrogen cooling accessory enabling operation between −150 and 550 °C using a modulated DSC cell or at up to 750 °C using a regular DSC cell. Elemental analyses were performed by Atlantic Microlabs, Norcross (GA).

Infrared spectra (600–4000 cm^{-1}) were obtained on a Bio-Rad FT-40 spectrophotometer in mineral-oil mulls. UV/Vis spectra were obtained on an HP 8952A diode array spectrometer.

X-ray crystal structure analysis: Crystallographic data (excluding structure factors) for the structures reported in this paper have been deposited with the Cambridge Crystallographic Data Center as supplementary publication no. CCDC-102234 (−45 °C) and CCDC-102090 (−179 °C). Copies of the data can be obtained free of charge on application to CCDC, 12 Union Road, Cambridge CB2 1EZ, UK (fax: (+44) 1223-336-033; e-mail: deposit@ccdc.cam.ac.uk).

Acknowledgments

The authors gratefully acknowledge support from the National Science Foundation (Grant No. CHE9320478) as well as technical assistance provided by Mathew Lam (University of Delaware).

[1] a) Proceedings of the Conference on Ferromagnetic and High Spin Molecular Based Materials, (Eds.: J. S. Miller, D. A. Dougherty), *Mol. Cryst. Liq. Cryst.* **1989**, *176*; b) Proceedings of the Conference on Molecular Magnetic Materials, O. Kahn, D. Gatteschi, J. S. Miller, F. Palacio (Eds.); c) *NATO ARW Molecular Magnetic Materials*, **1991**, *E198I*; d) Proceedings of the Conference on the Chemistry and Physics of Molecular Based Magnetic Materials, (Eds.: H. Iwamura, J. S. Miller), *Mol. Cryst. Liq. Cryst.* **1993**, *232/233*; e) Proceedings of the Conference on Molecule-Based Magnets, (Eds.: J. S. Miller, A. J. Epstein), *Mol. Cryst. Liq. Cryst.* **1995**, *271–274*; f) Proceedings of the Conference on Molecular-Based Magnets, (Eds.: K. Itoh, J. S. Miller, T. Takui), *Mol. Cryst. Liq. Cryst.* **1997**, *305/306*; g) *Molecular-based Magnetic Materials* (Eds.: M. M. Turnbull, T. Sugimoto, L. K. Thompson), *ACS Symposium Series No. 644*, American Chemical Society, Washington, DC, **1996**.

[2] Reviews: a) A. L. Buchachenko, *Russ. Chem. Rev.* **1990**, *59*, 307; *Usp. Khim.* **1990**, *59*, 529; b) O. Kahn, *Molecular Magnetism*, VCH, New York, **1993**; c) A. Caneschi, D. Gatteschi, R. Sessoli, P. Rey, *Acc. Chem. Res.* **1989**, *22*, 392; d) D. Gatteschi, *Adv. Mater.* **1994**, *6*, 635; e) J. S. Miller, A. J. Epstein, W. M. Reiff, *Acc. Chem. Res.* **1988**, *21*, 114; f) J. S. Miller, A. J. Epstein, W. M. Reiff, *Science* **1988**, *240*, 40 g) J. S. Miller, A. J. Epstein, W. M. Reiff, *Chem. Rev.* **1988**, *88*, 201; h) J. S. Miller, A. J. Epstein in *New Aspects of Organic Chemistry*, *Vol. 237*, (Eds.: Z. Yoshida, T. Shiba, Y. Ohsiro), VCH, New York, **1989**; i) J. S. Miller, A. J. Epstein, *Angew. Chem.* **1994**, *106*, 399; *Angew. Chem. Int. Ed. Engl.* **1994**, *33*, 385; j) J. S. Miller, A. J. Epstein, *Adv. Chem. Ser.* **1995**, *245*, 161; k) J. S. Miller, A. J. Epstein, *Chem. Eng. News* **1995**, *73*(40), 30.

[3] a) J. S. Miller, J. C. Calabrese, A. J. Epstein, R. W. Bigelow, J. H. Zhang, W. M. Reiff, *J. Chem. Soc. Chem. Commun.* **1986**, 1026; b) J. Miller, J. Calabrese, H. Rommelmann, S. Chittipeddi, J. Zhang, W. Reiff, A. Epstein, *J. Am. Chem. Soc.* **1987**, *109*, 769.

[4] J. Manriquez, G. Yee, R. S. Mclean, A. J. Epstein, J. S. Miller, *Science* **1991**, *252*, 1415; b) A. J. Epstein, J. S. Miller, in *Conjugated Polymers and Related Materials: The Interconnection of Chemical and Elec-*

tronic Structure, Proceedings of Nobel Symposium NS-81, Oxford University Press, Oxford, **1993**, p. 475; c) *La Chimica & La Industria*, **1993**, *75*, 185, 257; d) J. S. Miller, G. T. Yee, J. M. Manriquez, A. J. Epstein, in *Conjugated Polymers and Related Materials: The Interconnection of Chemical and Electronic Structure*, Proceedings of Nobel Symposium NS-81, Oxford University Press, Oxford, **1993**, p. 461; e) *La Chimica & La Industria*, **1992**, *74*, 845.

[5] a) J. S. Miller, J. C. Calabrese, R. S. Mclean, A. J. Epstein, *Adv. Mater.* **1992**, *4*, 498; b) P. Zhou, B. G. Morin, A. J. Epstein, R. S. McLean, J. S. Miller, *J. Appl. Phys.* **1993**, *73*, 6569.

[6] J. S. Miller, A. J. Epstein, *J. Chem. Soc. Chem. Commun*. **1998**, 1319.

[7] a) A. Böhm, C. Vazquez, R. S. McLean, J. C. Calabrese, S. E. Kalm, J. L. Manson, A. J. Epstein, J. S. Miller, *Inorg. Chem.* **1996**, *35*, 3083; b) K-i. Sugiura, A. Arif, D. K. Rittenberg, J. Schweizer, L. Öhrstrom, A. J. Epstein, J. S. Miller, *Chem. Eur. J.* **1997**, *3*, 138; c) E. J. Brandon, K-i. Sugiura, A. M. Arif, L. Liable-Sands, A. L. Rheingold, J. S. Miller, *Mol. Cryst. Liq. Cryst.* **1997**, *305*, 269; d) E. J. Brandon, B. M. Burkhart, R. D. Rogers, J. S. Miller, *Chem. Eur. J.* **1998**, *4*, 1938; e) E. J. Brandon, D. K. Rittenberg, A. M. Arif, J. S. Miller, *Inorg. Chem.* **1998**, *37*, 3376; f) E. J. Brandon, A. M. Arif, B. M. Burkhart, J. S. Miller, *Inorg. Chem.* **1998**, *37*, 2792.

[8] K. Sugiura, S. Mikami, T. Tanaka, M. Sawada, J. L. Manson, J. S. Miller, Y. Sakata, *Chem. Lett.* **1997**, 1071.

[9] a) K. Griesar, M. A. Anthanassopoulou, E. A. Soto Bustamante, Z. Tomkowicz, A. J. Zaleski, W. Haase, *Adv. Mater*. **1997**, *9*, 45; b) H. Winter, E. Dormann, R. Gompper, R. Janner, S. Kothrade, B. Wagner, H. Naarmann, *J. Magn. Magn. Mater*. **1995**, *140–144*, 1443; c) H. Winter, M. Klemen, W. Dormann, R. Gompper, R. Janner, S. Kothrade, B. Wagner, *Mol. Cryst. Liq. Cryst.* **1995**, *273*, 111.

[10] a) K. Nagai, T. Iyoda, A. Fujishima, K. Hashimoto, *Synth. Met.* **1997**, *85*, 1701; b) K. Nagai, T. Iyoda, A. Fujishima, K. Hashimoto, *Solid State Commun.* **1997**, *102*, 809; c) K. Nagai, T. Iyoda, A. Fujishima, K. Hashimoto, *Chem. Lett.* **1996**, 591.

[11] a) E. J. Brandon, C. Kollmar, J. S. Miller, *J. Am. Chem. Soc.* **1998**, *120*, 1822; b) J. S. Miller, E. J. Brandon, in *NATO ARW Supramolecular Engineering of Synthetic Metallic Materials: Conductors and Magnets*, *C518*, (Eds.: J. Veciana, C. Rovira, D. Amabilino), **1998**, p. 197.

[12] F. R. Longo, M. G. Finarelli, J. B. Kim, *J. Heterocycl. Chem.* **1969**, *6*, 927.

[13] C. K. Chang, F. Ebina, *J. Chem. Soc. Chem. Commun.* **1981**, 778.

[14] K. Kadish, C. Araullomcadams, B. Han, M. Franzen, *J. Am. Chem. Soc.* **1990**, *112*, 8364.

[15] a) P. Becker, P. Coppens, R. K. Ross, *J. Am. Chem. Soc.* **1973**, *95*, 7604; b) D. A. Dixon, J. S. Miller, *J. Am. Chem. Soc.* **1987**, *109*, 3656.

[16] J. S. Miller, *Adv. Mater.* **1998**, *10*, 1553.

[17] For example: a) J. Kirner, C. A. Reed, R. Scheidt, *J. Am. Chem. Soc.* **1977**, *99*, 1093; b) V. Day, R. Stultz, E. Tasset, R. Marianelli, *Inorg. Nucl. Chem. Lett.* **1975**, *11*, 505; c) R. Scheidt, K. Hatano, G. Rupprecht, P. Piciulo, *Inorg. Chem.* **1979**, *18*, 292.

[18] B. M. Burkhart, B. G. Morin, A. J. Epstein, J. C. Calabrese, J. S. Miller, M. Sundaralingham, in press.

[19] a) J. S. Miller, C. Vazquez, J. C. Calabrese, R. S. Mclean, A. J. Epstein, *Adv. Mater.* **1994**, *6*, 217; b) J. S. Miller, C. Vazquez, N. Jones, L. R. S. McLean, A. Epstein, *J. Mater. Chem.* **1995**, *5*, 707.

[20] J. Seiden, *Phys. Lett.* **1983**, *44*, L947.

[21] C. M. Wynn, M. A. Girtu, K. I. Sugiura, E. J. Brandon, J. L. Manson, J. S. Miller, A. J. Epstein, *Synth. Met.* **1997**, *85*, 1695.

[22] J. A. Mydosh, *Spin Glasses. An Experimental Introduction*, Taylor and Francis, London, **1993**.

Received: October 26, 1998 [F 1403]